

Dependence of naphthenic acid corrosion of SA106B on temperature and turbulence

Y F Shi¹, Q K Zheng¹, J Liu¹, L B Zhang², Z W Pan¹ and S X Rao^{1,3}

¹ School of mechanical engineering, Anhui university of technology, Ma'an'shan, 243002, P R China

² HuaiHai Industry group Co. Ltd, Changzhi, 046012, P R China

³ E-mail: snowdrio@126.com

Abstract. Analysis about the kinetic mechanism of Naphthenic Acid Corrosion (NAC) indicated that the natural logarithm of corrosion rate ($\ln r$) was proportional to negative reciprocal of temperature ($-1/T, K$), linear regression on the corrosion data in API581 and experiments both proved the linear relationship between $\ln r$ $-(-1/T, K)$ which could be applied to predicate the average corrosion rate under different temperature. Corrosion morphology observations proved the influence of turbulence on NAC, measurements on the maximum corrosion depth in different turbulence area indicated that in 7.5% turbulence area the corrosion depth could be 2-3 times of the corrosion depth in 2% turbulence area, existence of turbulence could lead to serious local NAC.

1. Introductions

Naphthenic Acid Corrosion (NAC) is a special corrosion mode mainly existed in high acid crude oil processing refineries, although NAC has been discovered for nearly one century, but up to now it keeps to be a reliability issue in the oil refineries.

Existing researches have confirmed the main corrosion mechanism and influencing factors of NAC, the main influencing factors are listed in figure 1 [1-3]. Temperature is the most important factor that could significantly influence NAC, NAC would not occur below 473.15K, as NAC is an endothermal reaction and high activation energy barrier could inhibit obvious NAC under low temperature. When temperature exceeds 673.15K, Most organic Naphthenic Acids (NA) would decompose and NAC vanishes [4-5].

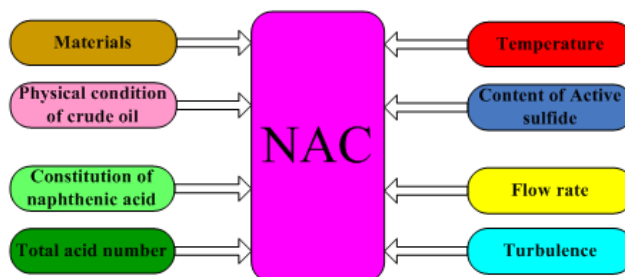


Figure 1. The main influencing factors of NAC.

Total acid number(TAN) is related with the content of NA in high acid crude oil. In fact NA is a complex mixture of hundreds of carboxylic acid, the content of NA could determine the NAC rate [6-7]. Available researches indicated that obvious NAC only occurred above TAN of 0.5mgKOH/g.

NA constitution of high acid crude oil from different origins is not the same. As mentioned above, NA is a complex mixture of various carboxylic acid, the corrosivity of each carboxylic acid is quite different which means the corrosivity of crude oil from different origins may differ obviously even under the same TAN. Researches by Omar indicated that the corrosivity of carboxylic acid depended on the solubility of iron naphthenate in crude oil[8].

Sulfides also exist in high acid crude oil, the existence of active sulfides could lead to sulfide corrosion, meanwhile active sulfides could influence NAC. Appropriate content of active sulfides may suppress NAC through forming an integrate sulfide film on the metal, but the content must be controlled accurately. If the content of active sulfide is too low, the sulfide film formed on the metal is not thick enough and imperfect, the incomplete sulfide film could not play enough protection role. Meanwhile too high content of active sulfides would cause serious sulfide corrosion [9-11].

Although existing researches had confirmed the main factors of NAC, but the mechanism of NAC still could not be determined [12], the dependence of corrosion rate on each influencing factor were not clear[13]. With the drying up of high quality crude oil, in the future high acid crude oil processing would be inevitable. Thus NAC should be further researched. Here the mechanism of NAC was discussed firstly, then the dependence of NAC rate on temperature and turbulence was researched.

2. Experiment preparations

2.1. Experimental materials and specimens

As ASME SA106B low carbon steel was widely used as pipeline material in oil refineries and the corrosion resistance of SA106B to NAC was poor, SA106B was selected as experimental material. SA106B was quenched and tempered, the metallurgical structure was shown in figure2. The nominal chemical compositions of SA106B were listed in table1. The specimens were machined to thin ring structure (As the model was shown in figure 3, the external diameter 18mm, internal diameter 3mm, thickness 3mm.).

Table 1. Chemical composition of test specimens (mass%).

| Alloy | C | Si | Mn | P | S | Cu | Ni | Fe |
|--------|------|------|------|-------|--------|--------|--------|---------|
| SA106B | 0.18 | 0.20 | 0.36 | ≤0.03 | ≤0.030 | ≤0.020 | ≤0.025 | Balance |

After experiments the specimens were taken out, first the specimens were rinsed by acetone to remove the oil remained on the surface, subsequently the specimens were cleaned by ultrasonic wave cleaner to remove the corrosion products, then the specimens were rinsed again by distilled water and dried for 24hours in glass dryer, finally the weight of the specimens were re-scaled and recorded. Then the weight loss of the specimens could be obtained. The average corrosion rate could be calculated by equation (1).

$$\text{Corrosion rate}(\text{mm/a}) = \frac{3650 \times (\text{Weight loss} / \text{g})}{\text{Density of metal}(\text{g/cm}^3) \times \text{Area}(\text{cm}^2) \times \text{time}(\text{day})} \quad (1)$$

2.2. Experimental parameters and procedures

As NAC mainly occurred in the temperature range from 473.15K to 673.15K, the experimental temperature selected were 513.15K, 533.15K, 553.15K, 573.15K, 593.15K, 613.15K and 633.15K, the corrosion time was controlled at 8 hours. In order to investigate the influence of turbulence on NAC, the specimens were installed at two flushing angles(0° and 90°) in pipelines(as shown in figure3).

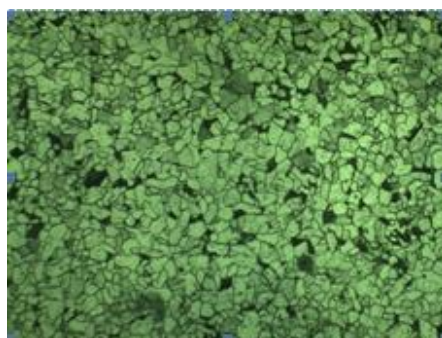


Figure 2. The metallurgical structure of SA106B.

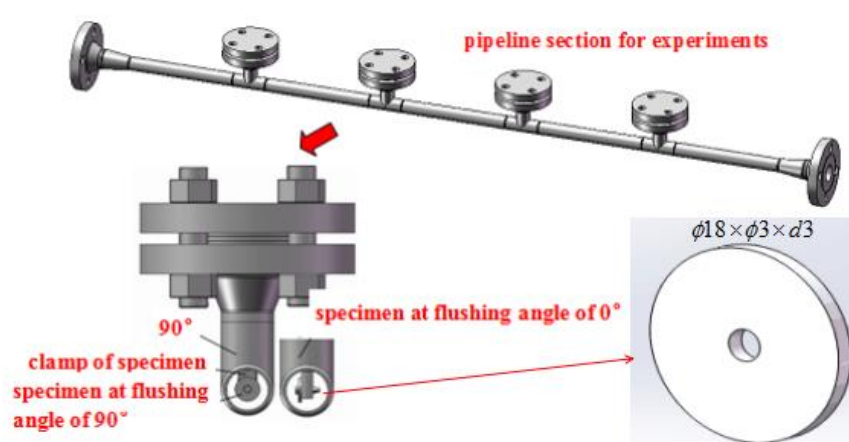


Figure 3. Installation diagram of specimens in the pipelines.

2.3. Analysis of turbulence and topography

Turbulence intensity was defined as the ratio of turbulent fluctuation velocity and average velocity, it could be calculated by equation (2). Here I is the turbulence intensity of fluid, Re is the Reynolds number and Re could be calculated by equation (3).

$$I = 0.16 * Re^{-1/8} \quad (2)$$

$$Re = \rho v d / \mu \quad (3)$$

ρ is the density of fluid, v is the flow velocity of fluid, d is the internal diameter of pipeline and μ is the dynamic viscosity of fluid (the values of the parameters above were listed in Table 2).

Table 2. The parameters needed in flow velocity and turbulence distribution simulation.

| ρ | v | d | μ |
|-----------------------|-------|------|-------------------------|
| 0.95g/cm ³ | 20m/s | 36mm | 1×10 ⁻² Pa·s |

3. Discussion on the mechanisms of NAC

3.1. Corrosion mechanism of NAC

The accepted corrosion mechanism of NAC is listed in the chemical reactions below.





Reaction(4) produces iron naphthenate which is oil-soluble and could be taken away by high flow velocity fluid, under most circumstances that is the reason that no obvious corrosion products remain on the metal. On the spots that highflow velocityand strong turbulence exists, the metal keeps corroding under flushing of high flow velocity fluid, finally streamline groove would be formed on the surface.

Reaction(5) indicates that existence of active sulfides could influence NAC, the active sulfides under high temperature could be transformed to H_2S , H_2S could react with iron and produces FeS , as FeS does not dissolve in the oil and could combine with the substrate tightly, if the content of active sulfides is appropriate, integrated FeS protection film could be formed on the substrate, the FeS protection film could insulate NA from the metal and suppress NAC to some extent, that is why NAC rate would decrease under some circumstances when active sulfides exist. However when the content of active sulfides is too low, the FeS protection film formed is not integrated, then NAC still exists, H_2S would react with iron naphthenate and release NA again as shown in reaction(6).

The mechanism above integrates the influence of active sulfide on NAC, but when no active sulfides exist, NAC still occurs. To uncover the corrosion law of NAC, the influence of active sulfide must be removed. In the following experiments no active sulfides were added, then only reaction(4) existed.

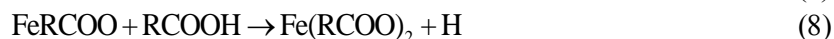
Some researchers thought that NAC belonged to electrochemical reaction, the fact was not true. As NAC occurs in crude oil instead of in water, the electro-conductibility of crude oil is less than $0.01\mu\text{s}/\text{cm}$, obviously lower than the electro-conductibility of pure water($0.05\mu\text{s}/\text{cm}$), meanwhile most of the iron naphthenate would ionize in crude oil. Generally NAC is a kind of pure chemical reaction instead of electrochemical reaction.

3.2. Kinetic mechanism of NAC

Up to now the kinetics mechanism of NAC is still indecisive, what is the control step of NAC needs to be confirmed.

In static laboratory experiments, the mass transfer, adsorption and desorption of reactants and resultants could be the control step.

On the spots that serious NAC exists, the flow velocity of fluid is quite high and strong turbulence exists, mass transfer, adsorption and desorption of reactants and resultants would not be the corrosion control step, the corrosion is controlled by the corrosion reaction itself. The total chemical reaction of pure NAC is listed in reaction (4), but in fact reaction(4) could be divided into several elementary reactions, here it is supposed that two elementary reactions existed (listed in equation (7) and in equation (8)).



Equation (7) and equation (8) indicated that only the first elementary reaction (equation (7)) was directly related with corrosion of metal, the second elementary reaction(equation (8)) only transformed the intermediates FeRCOO into final resultant Fe(RCOO)_2 . In pipelines crude oil flowed at high rate and the intermediates of equation (7) could be taken downstream and then transformed to final resultant as equation (8), so it sounded that corrosion was mainly controlled by the first elementary reaction, then the corrosion rate could be expressed as $r = k_1[\text{RCOOH}][\text{Fe}]$.

In the same refining pipelines the constitutions and TAN of crude oil keep steady, so the concentration of RCOOH could be supposed to be constant, the reactant of Fe was solid, the first elementary reaction could be considered as zero order reaction. Thus total NAC rate was only controlled by the rate constant k_1 of the first elementary reaction. According to Arrhenius equation $k_1 = A\exp(-E_a/RT)$, corrosion rate r was proportional to k_1 and $\exp(-E_a/RT)$. So it was deduced that the natural logarithm of corrosion rate ($\ln r$) was proportional to negative reciprocal of temperature ($-1/T, \text{K}$) and the slope of $\ln r - (-1/T)$ line was related to activation energy E_a .

4. Experiment results and discussion

4.1. Dependence of NAC rate on temperature

To verify the linear relationship between $\ln r$ and $(-1/T)$ deduced above, the naphthenic acid corrosion data at five different TAN levels ($\text{TAN} \leq 0.3$, $0.3 \leq \text{TAN} \leq 1.0$, $1.1 \leq \text{TAN} \leq 2.0$, $2.1 \leq \text{TAN} \leq 4.0$, $\text{TAN} \geq 4.0$) of low carbon steel and 1.25Cr in API581 were analyzed. The analysis results of corrosion data were shown in figure 4 and figure 5.

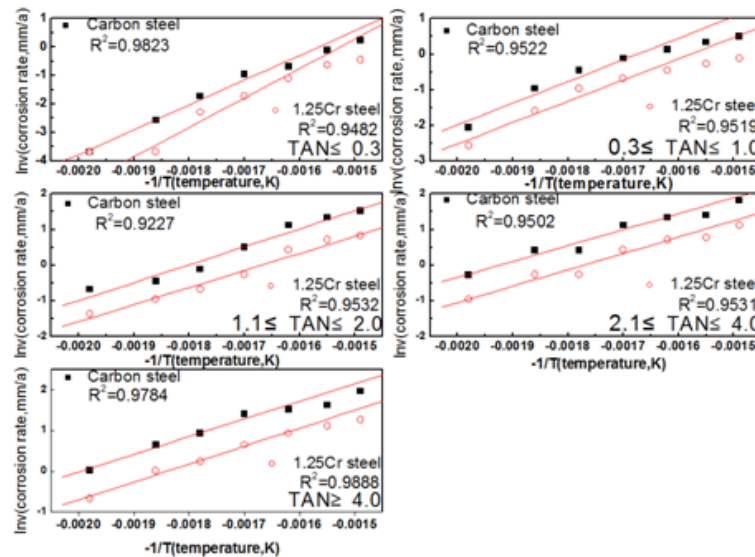


Figure 4. $\ln r$ and $(-1/T)$ of low carbon steel and 1.25Cr low alloy steel at different TAN (content of S $\leq 0.2\%$).

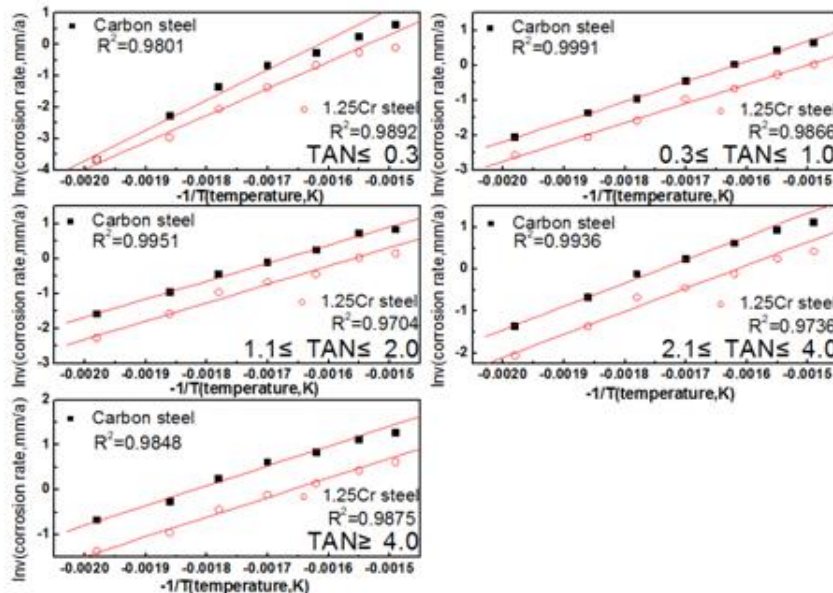


Figure 5. $\ln r$ and $(-1/T)$ of low carbon steel and 1.25Cr low alloy steel at different TAN (0.2% \leq content of S $\leq 0.6\%$).

Figure 4 and figure 5 indicated that the relationship between $\ln r$ and $(-1/T)$ of low carbon steel and 1.25Cr low alloy steel accorded with linear relation quite well, it was confirmed that linear relationship between $\ln r$ and $(-1/T)$ did exist.

As mentioned above the slope of $\ln r$ $-(-1/T)$ line was related with the activation energy E_a . After linear regression, the slope of all the fitting lines could be obtained. It was found that the slope of the fitting lines decreased with the increase of temperature and TAN, this phenomenon could be attributed to the fact that NA is a complex mixture of hundreds of carboxylic acid, with increasing temperature, more carboxylic acid participated in NAC.

To further prove the linear relationship between $\ln r$ and $(-1/T)$, naphthenic acid corrosion experiments of SA106B were carried out. The relationship between $\ln r$ and $(-1/T)$ was listed in figure 6, the experiment results also proved the linear relationship of $\ln r$ and $(-1/T)$. The linear relationship between $\ln r$ and $(-1/T)$ had been occasionally reported by some researchers, but those researchers did not find the reason why the linear relationship existed.

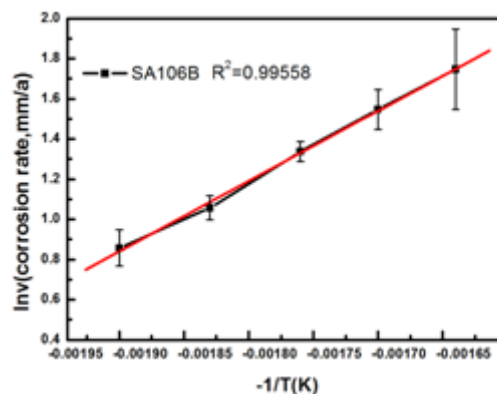


Figure 6. $\ln r$ and $(-1/T)$ of SA106B at TAN of 4.6mgKOH/g.

4.2. Dependence of NAC on flow rate and turbulence

4.2.1. Analysis of flow rate and turbulence around the specimens. As severe NAC occurred on the spots that high flow velocity and remarkable turbulence existed. The corrosion rate must be related with flow velocity and turbulence. In experiments two flushing angles were applied (0° and 90°) to create different turbulence distribution. To correlate NAC rate with flow velocity and turbulence, the flow velocity distribution and turbulence distribution must be simulated.

The inlet velocity of fluid was controlled at 20m/s, then the flow velocity distributions under two flushing angles were simulated and shown in figure 7 and figure 8. On the surface of 90° specimen in figure 7, due to the blockage of specimen, the flow velocity on the specimen was decreased to lower than 10m/s; while on the surface of 0° specimen in figure 8, the block effect was not so obvious, the flow velocity on the specimen was still close to 20m/s.

The specimens installed in the pipeline varied the direction of fluid flow, highly increased the flow velocity around the specimens and formed strong turbulence. In figure 8 the max flow velocity could exceed 45m/s which was much higher than the inlet velocity of 20m/s.

The turbulence distributions on the specimens under two flushing angles were simulated and shown in figure 9. From figure 9a it was confirmed that under flushing angle of 90° the highest turbulence existed in the central ring of the specimen, while under flushing angle of 0° the highest turbulence existed in the edge facing the flow direction (shown in figure 9b). On both specimens turbulence intensity could reach 7.5%.

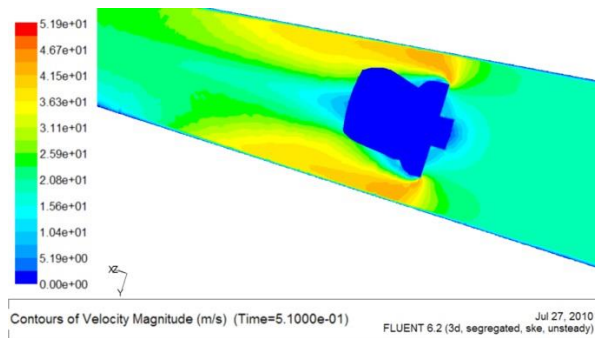


Figure 7. Flow velocity distribution around the specimens at 90°.

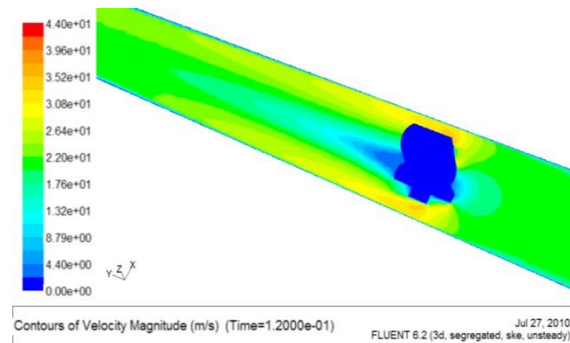


Figure 8. Flow velocity distribution around the specimens at 0°.

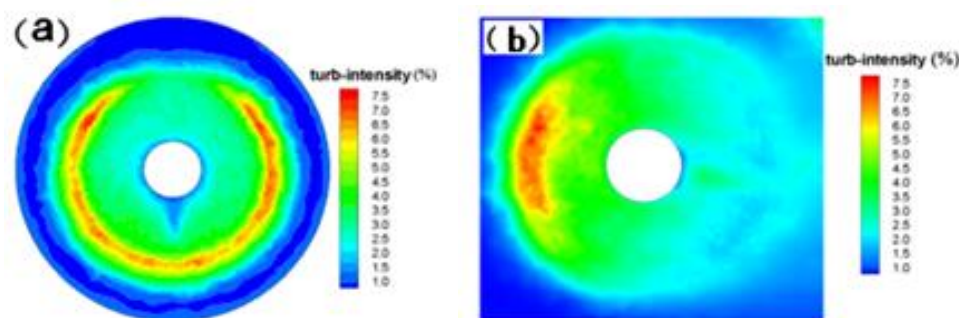


Figure 9. Turbulence distribution on the work area of the specimens (a- 90°, b- 0°)

4.2.2. Dependence of NAC rate on flow velocity and turbulence. As the turbulence intensity on the specimen was directly related with the inlet velocity of fluid, it was difficult to separate the influence of flow velocity and turbulence. As in straight pipelines no obvious turbulence existed, NAC was not serious even under high flow velocity, the corrosion morphology on the specimen was quite smooth and no obvious local NAC existed, it was deduced that the influence of flow velocity on NAC was mainly expressed in the increment of average corrosion rate. As the flow velocity distribution on the specimens under two flushing angle was quite different, the average corrosion rate under two flushing angle was compared with each other. Under most circumstances the corrosion rate under 90° was slightly higher than the corrosion rate under 0°, the max difference was limited in 20%. Even when the flow velocity of fluid was increased to 80m/s, the corrosion rate difference under two flushing angle was limited in 50%. That is to say, the increase of flow velocity could aggravate average NAC rate, but the influence was limited.

When no turbulence existed, NAC is almost an uniform corrosion, but when strong turbulence existed, the corrosion morphology was quite different. The corrosion morphology of SA106B at 513.15K under flushing angle of 90° was recorded and listed in figure 10. In figure 10a the ferrite grains could be distinguished easily, but the pearlites could not be obviously observed, this fact indicated that the pearlites dissolved preferentially in NA, as the turbulence intensity in inner ring was quite low (less than 2%), NAC was quite slight. In central ring the turbulence intensity was increased to 7%-8%, the corrosion was more obvious relative to the corrosion in inner ring, almost all the pearlites disappeared, most ferrite grains could still be distinguished, but some grain boundaries became fuzzy and some ferrite grains had been corroded (shown in figure 10b). In outer ring the turbulence intensity was about 5%, the corrosion morphology was similar to the morphology in central ring (shown in figure 10c).

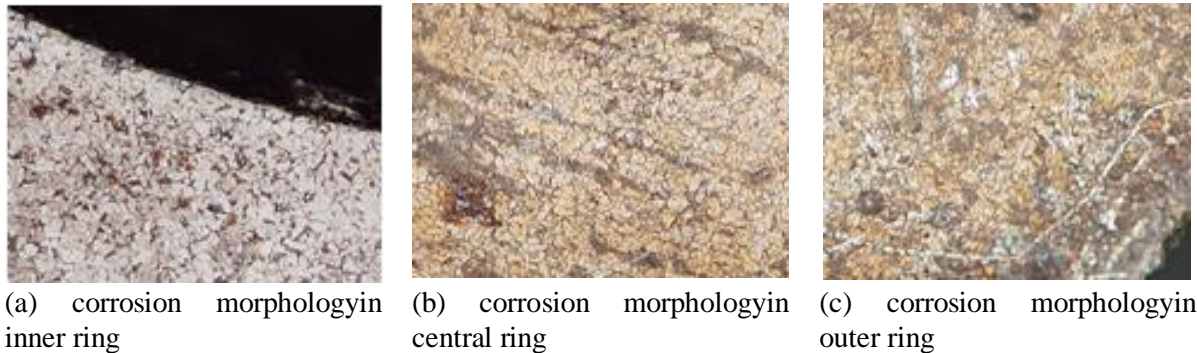
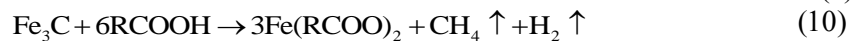


Figure 10. Corrosion morphology of SA106B at 513.15K under flushing angle of 90°.

The preferential dissolution of pearlites indicated pearlites were more sensitive to NAC, it is known that the main chemical constitution of pearlites is Fe_3C which is soluble in acids. In hydrochloric acid the pearlites would react with acid as equation (9). But NAC occurs in crude oil in which the content of water was quite low, NA would not ionize and could not react with pearlites as equation (9). Since active sulfides are not added in the experiments, the possible reaction between NA and pearlites could be expressed by equation (10).



The ferrites could also react with NA, but the corrosion rate was much lower than the corrosion rate of pearlites in NA. From the corrosion difference in different turbulence distribution area, it was confirmed that turbulence could aggravate NAC.

When the temperature was increased to 553.15K, NAC became more serious relative to 513.15K. In inner ring as the turbulence intensity was quite low, although the pearlites dissolved completely, but most ferrites still kept integrate, grain boundaries could still be distinguished. In central ring the pearlites and ferrites corroded seriously, no grain boundaries could be seen, a clear boundary (dot dash line shown in figure 11a) could be observed between the inner ring and central ring due to the different corrosion severity induced by turbulence intensity distribution. The same phenomenon existed between central ring and outer ring, as the corrosion rate at 553.15K increased obviously and the corrosion rate in central ring and outer ring differed obviously, clear boundary (dot dash line shown in figure 11b) also formed between central ring and outer ring.

The corrosion morphology on the ring specimen could be related with the turbulence distribution in figure 8 directly. The boundaries in different area on the specimen further proved the significant influence of turbulence on corrosion rate.

Even when the temperature was increased to 593.15K, some ferrite grains in inner ring kept quite integrate and some grain boundaries could be observed (shown in figure 12a). But in central ring most ferrite grains had disappeared (shown in figure 12b), corrosion in central ring became quite serious.

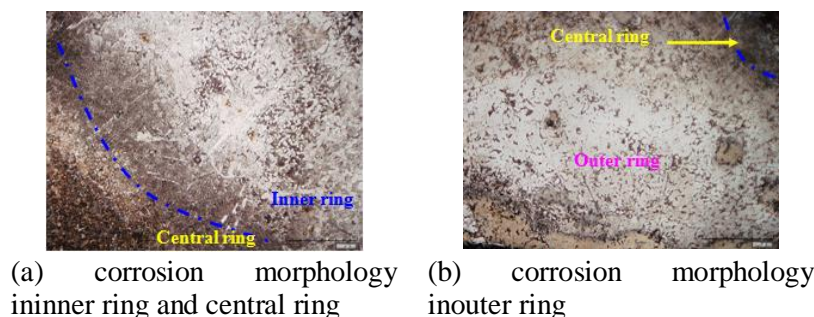


Figure 11. Corrosion morphology of SA106B at 553.15K under flushing angle of 90°.

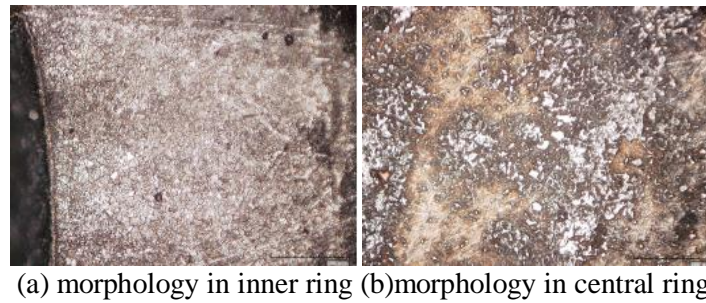
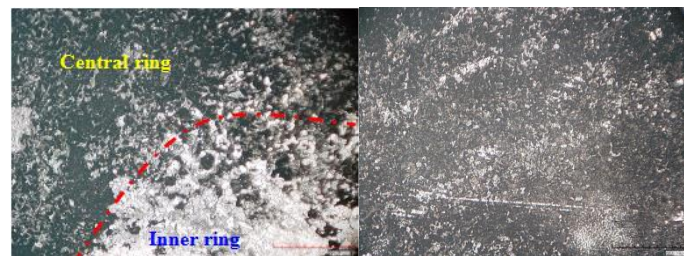


Figure 12. Corrosion morphology of SA106B at 593.15K under flushing angle of 90°.

When temperature was increased to 633.15K, the corrosion became more serious, in inner ring most ferrite grains had been corroded (shown in figure 13a), in central ring almost all the ferrite grains had disappeared and no grain boundaries could be observed (shown in figure 13b).



(a) morphology in inner ring and central ring (b) morphology in central ring

Figure 13. Corrosion morphology of SA106B at 633.15K under flushing angle of 90°.

Although significant influence of turbulence on local NAC had been confirmed through corrosion morphology analysis, the dependence of local corrosion rate on turbulence had not been determined quantitatively. In local corrosion, the maximum corrosion depth was the most important indicator. To uncover the relationship between maximum corrosion depth and turbulence intensity, the maximum corrosion depth in different turbulence area must be analyzed.

As the experimental corrosion time was controlled at 8 hours, the average corrosion rate could be transformed to average corrosion depth DA in 8 hours. Maximum corrosion depth in different turbulence intensity area were measured and listed in Table 3. Table 3 indicated that the ratio between maximum corrosion depth in 7.5% turbulence area (DM,7.5%) and 2% turbulence area (DM,2%) increased with temperature, this phenomenon indicated that under action of turbulence, local NAC became more serious with increasing temperature, the maximum corrosion depth in 7.5% turbulence area could be 2-3 times of the corrosion depth in 2% turbulence area.

Table 3. Influence of turbulence on maximum corrosion depth.

| Temperature | 513.15K | 553.15K | 593.15K | 633.15K |
|--|---------|---------|---------|---------|
| Average corrosion rate (mm/a) | 2.52 | 3.94 | 6.89 | 5.81 |
| Average corrosion depth(μm), DA | 2.30 | 3.6 | 6.29 | 5.30 |
| Maximum corrosion depth in 2% turbulence area (mm/a) , DM,2% | 3.71 | 4.02 | 4.67 | 4.90 |
| Maximum corrosion depth in 7.5% turbulence area (mm/a) , DM,7.5% | 5.73 | 8.69 | 12.03 | 13.78 |
| Ratio between DM,7.5% and DA | 2.49 | 2.41 | 1.91 | 2.6 |
| Ratio between DM,7.5% and DM,2% | 1.54 | 2.16 | 2.58 | 2.81 |

Restricted by the safety of experimental devices, the experimental time had to be controlled at 8 hours, if the corrosion time was long enough, the corrosion rate difference on the specimen would lead to the formation of groove, this fact could explain why streamline grooves often appears in NAC.

5. Conclusion

(1) Analysis about kinetic mechanism of NAC indicated natural logarithm of corrosion rate ($\ln r$) was proportional to negative reciprocal of temperature ($-1/T, K$). Linear regression on the corrosion data in API581 and experiments proved the existence of the linear relationship between $\ln r$ and $-1/T$, this linear relationship could be used to predicate the average corrosion rate under different temperature.

(2) The corrosion morphology indicated that preferential corrosion of pearlites existed, when NAC occurred, corrosion rate of pearlites was much higher than the corrosion rate of ferrites. Meanwhile the corrosion morphology proved the influence of turbulence on local NAC, in high turbulence area local NAC became serious.

(3) Maximum corrosion depth in different turbulence area indicated that in 7.5% turbulence area the maximum corrosion depth could be 2-3 times of the corrosion depth in 2% turbulence area. The ratio between DM_{7.5%} and DM_{2%} increased with increasing temperature. The relationship between turbulence and local corrosion depth could be applied to predicate the maximum corrosion depth in local NAC.

Acknowledgements

Thanks for the support by National High Technology Research and Development Program of China (No.2012AA040103) and Anhui province natural science research project (KJ2016SD09).

Reference

- [1] Qu D R, Zheng Y G, Jing H M, Yao Z M and Ke W 2006 High temperature naphthenic acid corrosion and sulphidic corrosion of Q235 and 5Cr1/2Mo steels in synthetic refining media *Corrosion Science* **48** 1960-1985
- [2] Wu X Q, Jing H M, Zheng Y G, Yao Z M and Ke W 2004 Erosion Corrosion of Various Oil refining Materials in Naphthenic acid *Wear* **256** 133-144
- [3] Slavcheva E, Shone B and Turbull A 1999 Review of naphthenic acid corrosion in oil refining *British Corrosion Journal* **34** 125-131
- [4] Rao S X, Zhou Y, AiZhibin, Pan Z W, Cen Y W and Chen X D 2014 High temperature Naphthenic Acid Corrosion of SA210C and A335-P5 *Materials and Corrosion* **65** 619-625
- [5] Wu X Q, Jing H M, Zheng Y G, Yao Z M and Ke W 2004 Study on high-temperature naphthenic acid corrosion and erosion-corrosion of aluminized carbon steel *Journal of Materials Science* **39** 975-985
- [6] Nugent M J, Dobis J D 1998 Experience with Naphthenic Acid Corrosion in low TAN Crudes *Corrosion 98 Houston NACE International* **577**
- [7] OmarYepez 2005 Influence of Different Sulfur Compounds on Corrosion Due to Naphthenic Acid *Fuel* **84** 97-104
- [8] OmarYepez 2007 On the Chemical Reaction between Carboxylic Acids and Iron, Including Special case of Naphthenic Acid *Fuel* **86** 1162-1168
- [9] Craig H L 1996 Temperature and Velocity Effects in Naphthenic Acid Corrosion *Corrosion 96 Houston NACE International* **603**
- [10] Liu G Q, Zheng Y G, Jiang S L, Jing J H, Dong W J, Zeng H and Si P X 2015 Stability and Erosion Corrosion Behavior of Corrosion Product Film of Q235 Carbon Steel and Cr5Mo Low Alloy Steel in Simulated Oil Refinery Media *Journal of Chinese Society for Corrosion and Protection* **35** 122-128
- [11] Peng J, Nesic S and Wolf H A 2015 Analysis of corrosion scales formed on steel at high temperatures in hydrocarbons containing model naphthenic acids and sulfur compounds *Surface and Interface Analysis* **47** 454-465

- [12] Rebak R B 2011 Sulfidic corrosion in refineries a review *Corros Rev* **29** 123-133
- [13] Trasatti S P, Gabetta G 2006 Study of naphthenic acid corrosion by neural network *Science and Technology* **4** 200-211